OPEN

Citation: Cell Death and Disease (2014) 5, e984; doi:10.1038/cddis.2013.513

www.nature.com/cddis

Mitochondrial dysfunction, oxidative stress, and neurodegeneration elicited by a bacterial metabolite in a *C. elegans* Parkinson's model

A Ray[1], BA Martinez[1], LA Berkowitz[1], GA Caldwell[1,2] and KA Caldwell*[,1,2]

Genetic and idiopathic forms of Parkinson's disease (PD) are characterized by loss of dopamine (DA) neurons and typically the formation of protein inclusions containing the alpha-synuclein (α-syn) protein. Environmental contributors to PD remain largely unresolved but toxins, such as paraquat or rotenone, represent well-studied enhancers of susceptibility. Previously, we reported that a bacterial metabolite produced by *Streptomyces venezuelae* caused age- and dose-dependent DA neurodegeneration in *Caenorhabditis elegans* and human SH-SY5Y neurons. We hypothesized that this metabolite from a common soil bacterium could enhance neurodegeneration in combination with PD susceptibility gene mutations or toxicants. Here, we report that exposure to the metabolite in *C. elegans* DA neurons expressing human α-syn or LRRK2 G2019S exacerbates neurodegeneration. Using the PD toxin models 6-hydroxydopamine and rotenone, we demonstrate that exposure to more than one environmental risk factor has an additive effect in eliciting DA neurodegeneration. Evidence suggests that PD-related toxicants cause mitochondrial dysfunction, thus we examined the impact of the metabolite on mitochondrial activity and oxidative stress. An *ex vivo* assay of *C. elegans* extracts revealed that this metabolite causes excessive production of reactive oxygen species. Likewise, enhanced expression of a superoxide dismutase reporter was observed *in vivo*. The anti-oxidant probucol fully rescued metabolite-induced DA neurodegeneration, as well. Interestingly, the stress-responsive FOXO transcription factor DAF-16 was activated following exposure to the metabolite. Through further mechanistic analysis, we discerned the mitochondrial defects associated with metabolite exposure included adenosine triphosphate impairment and upregulation of the mitochondrial unfolded protein response. Metabolite-induced toxicity in DA neurons was rescued by complex I activators. RNA interference (RNAi) knockdown of mitochondrial complex I subunits resulted in rescue of metabolite-induced toxicity in DA neurons. Taken together, our characterization of cellular responses to the *S. venezuelae* metabolite indicates that this putative environmental trigger of neurotoxicity may cause cell death, in part, through mitochondrial dysfunction and oxidative stress.

Cell Death and Disease (2014) **5,** e984; doi:10.1038/cddis.2013.513; published online 9 January 2014
Subject Category: Neuroscience

Parkinson's disease (PD) is associated with dopaminergic neurodegeneration. Pathologically, this disease involves accumulation of the alpha-synuclein (α-syn) protein within proteineous inclusions called Lewy Bodies.[1] Current neurodegeneration research is focused on identification of the causative factors and underlying mechanisms. Around 10% of PD cases are caused by genetic factors. Unknown factors, including environmental exposures (heavy metals and agricultural chemicals such as paraquat and rotenone), are associated with most cases of parkinsonism.[2–6] There is also a higher incidence of PD in rural areas where the odds ratio cannot be completely accounted for by the level of toxic exposures often encountered by the use of chemicals in farming.[7] Associated with rural living, individuals exhibit a much greater interaction with the surrounding terrestrial environment through mechanisms such as well water consumption, farming, gardening, and/or living on dirt floors.

Streptomyces are a ubiquitous soil bacterial genus that have large genomes and produce a variety of secondary metabolites, including compounds that cause mitochondrial defects.[8] Evidence suggests that PD-related toxicants cause oxidative stress and mitochondrial dysfunction, which can lead to parkinsonism in animals.[9–11] In previous work, we reported that a bacterial metabolite produced by *Streptomyces venezuelae* caused age- and dose-dependent dopamine (DA) neurodegeneration in *Caenorhabditis elegans* and dose-dependent degeneration of human DA producing SH-SY5Y cells.[12] Thus, this metabolite might represent a

[1]Department of Biological Sciences, The University of Alabama, Tuscaloosa, AL, USA and [2]Departments of Neurobiology and Neurology, Center for Neurodegeneration and Experimental Therapeutics, University of Alabama at Birmingham, Birmingham, AL, USA
*Corresponding author: K Caldwell, Department of Biological Sciences, The University of Alabama, Tuscaloosa, AL 35487-0344, USA. Tel: +1 205 348 4021; Fax: +1 205 348 1786; E-mail: kcaldwel@bama.ua.edu
Keywords: ROS; dopamine; neurotoxin; Streptomyces
Abbreviations: 6-OHDA, 6-hydroxydopamine; α-syn, alpha synuclein; DA, dopamine; DβHB, D-beta hydroxybutyrate; EtAc, ethyl acetate; EV, empty vector; GFP, green fluorescent protein; PD, Parkinson's disease; RNAi, RNA interference; ROS, reactive oxygen species; UPR^{ER}, endoplasmic reticulum unfolded protein response; UPR^{mt}, mitochondrial unfolded protein response; UPS, ubiquitin proteasome system
Received 29.7.13; revised 18.11.13; accepted 20.11.13; Edited by E Baehrecke

previously uncharacterized environmental contributor to neurodegeneration.

Here, we extend the mechanistic analysis of this novel environmental effector of neurodegeneration to report that exposure to the *S. venezuelae* metabolite causes excessive production of reactive oxygen species (ROS) in *C. elegans*, as shown by a cellular reporter for superoxide dismutase and an *in vitro* biochemical assay. Likewise, the mitochondrial unfolded protein response (UPR^{mt}) pathway was upregulated and adenosine triphosphate (ATP) production impaired in response to metabolite exposure. In combinational studies using additional chemical and genetic modifiers associated with PD, we determined that metabolite exposure enhanced susceptibility to cell death. Moreover, we discerned that the mechanism of action involves targeting of mitochondrial complex I, and that antioxidant treatment rescues DA neurodegeneration. Taken together, these data provide a plausible underlying mechanism involved in *S. venezuelae* metabolite-induced toxicity.

Results

***S. venezuelae* metabolite exposure causes oxidative stress in *C. elegans*.** As previously reported,[12] the neurotoxic compound under investigation is a small secondary product (molecular weight <300) isolated following growth of *S. venezuelae* to the stationary phase in liquid culture where the compound is present in spent media. The *S. venezuelae* conditioned medium was extracted in dichloromethane (DCM), and ethyl acetate (EtAc) solvent was used to reconstitute the compound following partitioning, indicating that it is amphipathic. We have calculated an almost 100% recovery rate from this extraction (data not shown). Hereafter, we use the term metabolite to refer to this compound. EtAc is used as a negative (solvent) control in all experiments and does not cause a significant DA neurodegeneration.

To determine whether the metabolite increases ROS production *in vivo*, we examined *C. elegans* expressing an established oxidative stress-inducible reporter, *sod-3*::GFP, where green fluorescent protein (GFP) is driven under the endogenous *sod-3* gene promoter.[13] *sod-3* encodes a mitochondrial superoxide dismutase enzyme, which is thought to protect against oxidative stress. Worms treated with the metabolite exhibited a significant upregulation of *sod-3*::GFP expression compared with EtAc solvent control (Figures 1a–d). RNA interference (RNAi) depletion of *daf-2*, the *C. elegans* insulin/IGF receptor ortholog, was used as a positive control[14] (Figures 1a and d).

ROS production in response to the metabolite was also examined in *C. elegans* using an *ex vivo* 2,7-dichlorofluorescein diacetate (DCF-DA) assay.[15] Worms treated with either the *S. venezuelae* metabolite, 100 μM paraquat (positive control), or EtAc solvent were analyzed at day 7, day 10, and day 12 of exposure because DA neurodegeneration is observed following metabolite exposure at these time points.[12] The results showed significantly increased ROS production in metabolite- and paraquat-exposed worms at all days analyzed. Figure 1e displays day 7 data (days 10 and 12 are not shown).

Previously, we reported that exposure to the *S. venezuelae* metabolite caused DA neurodegeneration.[12] Treatment with 1 mM probucol, an anti-oxidant, fully rescued metabolite-induced DA neurodegeneration (Figures 1f–j). The protection by probucol indicates that free radical generation contributes to *S. venezuelae* metabolite toxicity. Thus, these data suggest that the *S. venezuelae* metabolite induces oxidative stress that, in turn, contributes to neuronal cell death.

Because *sod-3* is under the direct control of DAF-16, we sought to determine whether the DAF-16 transcription factor could be induced to translocate to the nucleus in response to metabolite treatment.[16] When compared with solvent treatment alone, we found that DAF-16 significantly accumulates within nuclei when animals are treated with metabolite or challenged with *daf-2* knockdown (Figures 2a and b). The nuclear accumulation observed could be related to increased ROS, because DAF-16 is a known stress-associated transcription factor induced by ROS, however, DAF-16 also responds to other stressors.[17]

In mammals, NRF-2 is the major ROS and detoxification transcription factor.[18] The *C. elegans* NRF-2 homolog, SKN-1, can be translocated to the nucleus by a variety of sources including pathogens and ROS.[19,20] However, when put to direct observation, SKN-1 failed to change its intracellular localization in response to metabolite treatment (data not shown), indicating that the ROS produced by the metabolite in *C. elegans* may not be sensed by the SKN-1 machinery.

***S. venezuelae* metabolite toxicity causes mitochondrial dysfunction.** Mitochondria are known to be a major source of ROS and perturbations that affect their metabolic activity can further promote the build-up of ROS and lead to complexities within the mitochondria such as an accumulation of misfolded proteins.[21] This subsequently triggers a stress-response pathway referred to as the UPR^{mt}, which activates transcription of mitochondrial chaperone genes to promote protein homeostasis. In *C. elegans*, this can be monitored in a strain expressing *hsp-6*::GFP,[22] where HSP-6 is a nuclear encoded mitochondrial chaperone and GFP is driven by the *hsp-6* promoter. *S. venezuelae* metabolite exposure caused an upregulation of *hsp-6*::GFP in day 4 worms when compared with solvent control (Figures 3a–c). RNAi depletion of *mev-1*, a *C. elegans* ortholog of a mitochondrial electron transport chain complex II subunit, was used as a positive control for increased *hsp-6* activation[23] (Figure 3a).

To investigate whether the *S. venezuelae* metabolite impacts mitochondrial respiratory chain activity (complex I–IV), ATP levels were measured in *C. elegans* extracts treated with either EtAc solvent control or *S. venezuelae* metabolite. A metabolic product of the neurotoxin MPTP [1-methyl-4-phenylpyridinium ($MPP+$)], which was shown to significantly decrease ATP production in a previous *C. elegans* study, was used as a positive control.[24] Our results showed that worms exposed to the *S. venezuelae* metabolite or $MPP+$ displayed significantly lower overall levels of ATP as compared with the solvent control (Figure 3d). Taken together, exposure to the *S. venezuelae* metabolite caused reduction in ATP levels, upregulation of

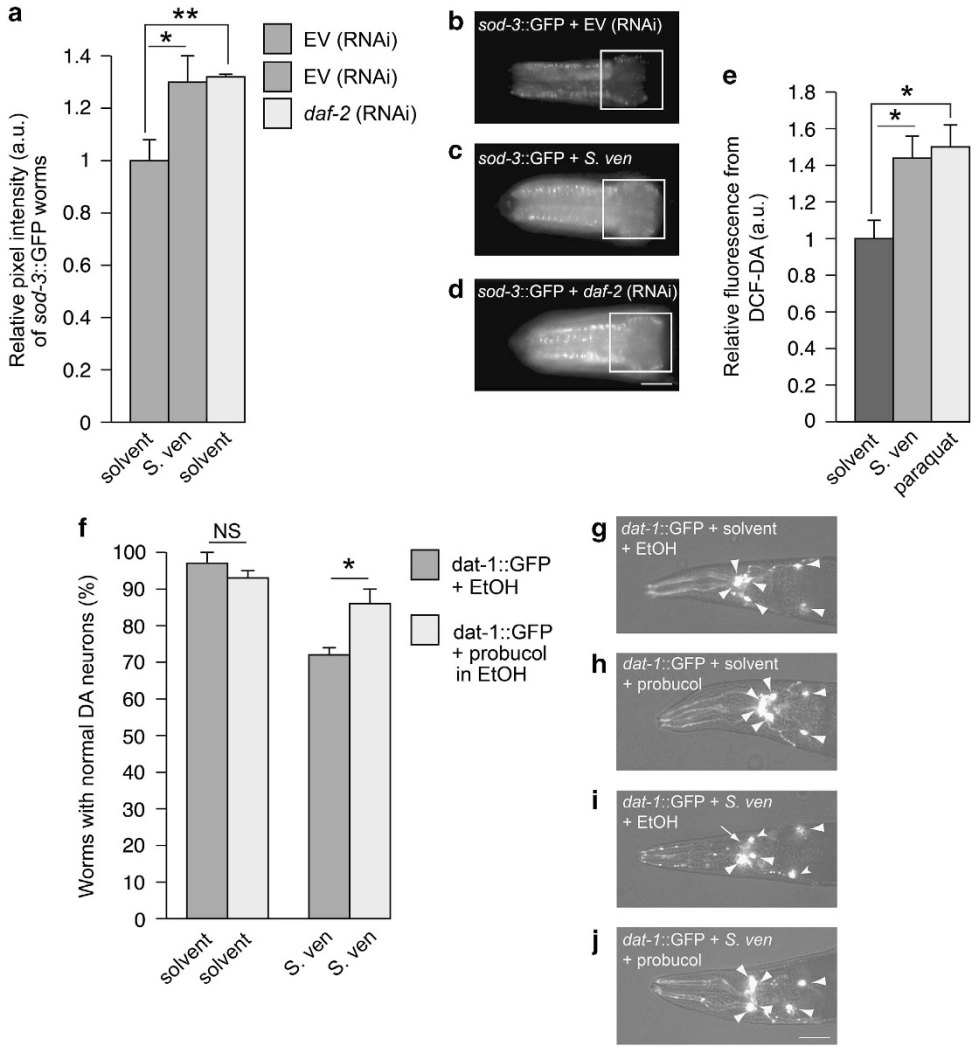

Figure 1 *S. venezuelae* metabolite causes oxidative stress in *C. elegans*. (**a**) *S. venezuelae* (*S. ven*) metabolite caused an upregulation of *sod-3*::GFP expression, an indicator of oxidative stress, in empty vector (EV) RNAi-treated worms when compared with worms exposed to solvent only, as quantitated using pixel intensities as described in (**b**–**d**). When compared with metabolite exposure, RNAi knockdown of *daf-2*, used as a positive control, expressed similar levels of *sod-3*::GFP. Values are the mean ± S.D. of 3 experiments where 30 animals were analyzed per replicate (*$P<0.05$; **$P<0.01$; one-way ANOVA). The values were normalized to the untreated solvent control. (**b**–**d**) Representative worm images for each of the treatments described in (**a**) where pixel intensities were measured in a 100 × 100 μm region at the anterior bulb of the pharynx. The white box shows the region of GFP measured in all animals. (**e**) *S. venezuelae* metabolite and 100 μM paraquat (positive control) significantly increased the amount of intracellular ROS compared with solvent control. Worms were evaluated using a DCF-DA assay by examining extracts (*$P<0.01$; one-way ANOVA; $n=3$ independent experiments). The values were normalized to the untreated solvent control. (**f**) Treatment with 1 mM probucol (dissolved in ethanol), an anti-oxidant, significantly rescued the *S. venezuelae*-induced neurotoxicity in DA neurons compared with metabolite treatment alone (*$P<0.01$; Student's *t*-test; $n=3$ independent experiments). (**g**–**j**) Representative images of the probucol experiment described in (**g**). All *C. elegans* (strain BY200) express GFP specifically in the six anterior DA neurons. In all images, large arrowheads show intact dopaminergic neuron cell bodies. Arrows indicate areas where dopaminergic neurons have degenerated. Small arrowheads indicate cell body degeneration. (**g**) Exposure to EtAc and ethanol (solvent for probucol) did not result in DA neuron loss. (**h**) The addition of probucol did not cause neurotoxicity, as evidenced by intact DA neurons. (**i**) *S. venezuelae* metabolite exposure caused substantial degeneration of cell processes, as displayed throughout the processes. Further, two of the cell bodies are degenerating and one is missing in this representative worm. (**j**) Probucol rescues *S. venezuelae*-induced DA neuronal toxicity, as shown in this *C. elegans* example. Magnification bars = 50 μm

UPR^{mt}, and production of ROS, revealing a role in mitochondrial dysfunction. These properties of the *S. venezuelae* metabolite are mechanistically similar to other environmental neurotoxins such as rotenone and paraquat.[9,11]

***S. venezuelae* metabolite toxicity involves mitochondria complex I.** Previously, it was demonstrated that the environmental toxins, rotenone and paraquat, as well as the experimental toxin model, 6-hydroxydopamine (6-OHDA), inhibit complex I of the mitochondria.[11,25,26] Our results indicating that exposure to the *S. venezuelae* metabolite caused impairment of mitochondrial function led us to further investigate whether this metabolite targets complex I. Here, we explored whether two chemicals that rescue complex I deficiency would provide protection against *S. venezuelae*-induced DA neurodegeneration. Riboflavin is an activator of mitochondrial complex I (NADH dehydrogenase) and D-beta-hydroxybutyrate (DβHB) is a complex II activator

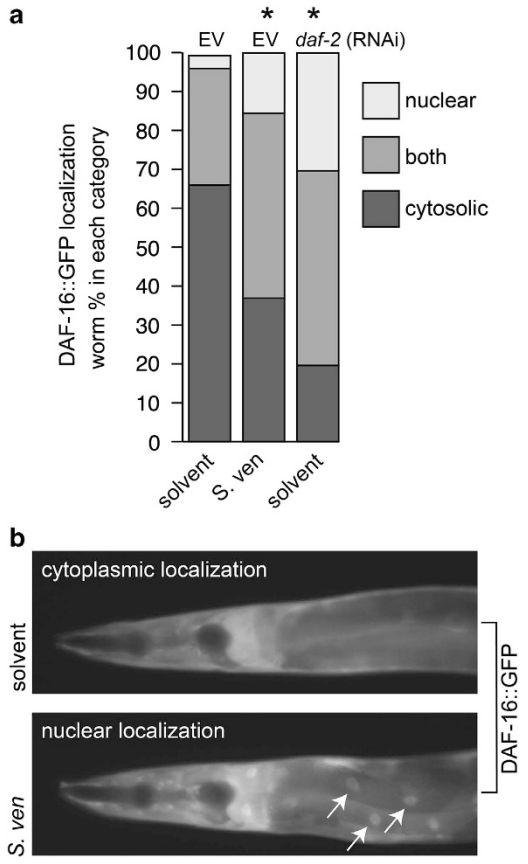

Figure 2 Effect of *S. venezuelae* metabolite on DAF-16 localization. (**a**) Stacked graph representing the percentage of *C. elegans* with DAF-16::GFP localization in the nucleus, cytoplasm, or both. *S. venezuelae* exposure promotes nuclear translocation of DAF-16::GFP in a manner similar to *daf-2* (RNAi), where both treatments were significantly different from EV solvent control (*$P<0.05$; one-way ANOVA; $n=3$ independent experiments with 30 animals/experiment). (**b**) Representative images of DAF-16::GFP localization in the cytoplasm and nucleus (arrows) following treatment with EtAc solvent and metabolite, respectively

(succinate dehydrogenase) that rescues complex I defects by a complex II-dependent mechanism.[27–29] In these experiments, riboflavin treatment significantly rescued *S. venezuelae* neurotoxicity (Figures 4a, c, and d). Similarly, treatment with DβHB significantly protected DA neurons from *S. venezuelae* metabolite-induced degeneration (Figures 4b, c, and e).

To further investigate the involvement of mitochondrial electron transport chain, we performed RNAi knockdown of mitochondrial genes, *gas-1* and *nuo-1* (subunits of complex I) and *mev-1* (subunit of complex II) specifically in DA neurons, and assayed for neurodegeneration using DA neuron-specific RNAi.[30] Depletion of these gene products without metabolite did not result in DA neurodegeneration (Figure 4f). Notably, addition of metabolite also did not cause DA neurodegeneration in either of the complex I gene knockdown conditions while the metabolite did cause degeneration in mock, empty vector (EV) RNAi conditions. Therefore, this experiment provides evidence that complex I is impaired by the metabolite. Conversely, knockdown of the complex II subunit, *mev-1*, resulted in a significant neurodegeneration compared with control (Figure 4f). Moreover, RNAi knockdown of complex I genes resulted in rescue of metabolite-induced DA neurodegeneration compared with mock RNAi treated with metabolite (Figure 4f). These results, together with the neuroprotection afforded by riboflavin and DβHB, suggest that complex I is involved in *S. venezuelae* metabolite-induced neurotoxicity. This complex I-specific effect could be due to the excessive production of ROS following metabolite exposure.

Mitochondrial complex I function may be decreased by α-syn,[31] a protein that when overexpressed or mutated, can lead to familial PD. Overexpression of α-syn is often used to induce neurodegeneration in animal models. In *C. elegans*, dopaminergic neurons undergo age-dependent neurodegeneration following human α-syn overexpression.[32] We exposed transgenic α-syn worms to the metabolite and discovered that the DA neurons showed enhanced degeneration to metabolite treatment (Figures 5a–c). Furthermore, α-syn-expressing worms exposed to metabolite displayed significantly more DA neurodegeneration than metabolite-treated animals expressing GFP only in DA neurons (Figure 5a). Thus, the compromised genetic background in the DA neurons of these animals rendered them more susceptible to secondary neurotoxicity *via* metabolite exposure.

In post-mortem human brains, mitochondrial accumulated α-syn was shown to interfere with complex I.[31] Furthermore, *in vitro* studies demonstrated that α-syn directly associates with mitochondrial membranes and causes mitochondrial fragmentation.[33] In this regard, we sought to evaluate whether there was an additive effect from the metabolite in neurons compromised from both α-syn overexpression and reduced complex I or II function through RNAi knockdown. Without metabolite susceptibility to DA neurodegeneration was significantly enhanced following RNAi knockdown of any one of these three genes beginning at day 6 compared with EV control in α-syn-expressing worms (Figure 5d). Metabolite exposure of α-syn-expressing *C. elegans* that were also treated with *gas-1* or *mev-1* (RNAi) did not result in enhanced DA neurodegeneration (Figure 5d). However, metabolite exposure of these worms treated with *nuo-1* (RNAi) resulted in enhanced neurodegeneration compared with *nuo-1* (RNAi) solvent control worms. Also, DA neurodegeneration was exacerbated by *nuo-1* (RNAi) *versus* EV control when treated with metabolite (Figure 5d). These data suggest that α-syn-expressing DA neurons treated with metabolite treated are more vulnerable to *nuo-1* knockdown. In general, mechanisms associated with α-syn and complex I gene interactions are not fully understood. Thus, the effect observed with our results in Figure 5d (*versus* Figure 4f) could be a result of direct or indirect interactions between metabolite, α-syn and mitochondrial components.

Another familial form of PD, mutation in LRRK2 (G2019S), has been shown to impact mitochondrial function whereby mitochondrial membrane potential and intracellular ATP production were impaired.[34] Studies in nematodes and mice have shown that this LRRK2 mutation can increase kinase activity and cause neuronal toxicity.[35] Thus, we examined the effect of metabolite using the LRRK2 G2019S mutation in *C. elegans*. The metabolite significantly enhanced DA neurotoxicity compared with solvent control (Figure 5e).

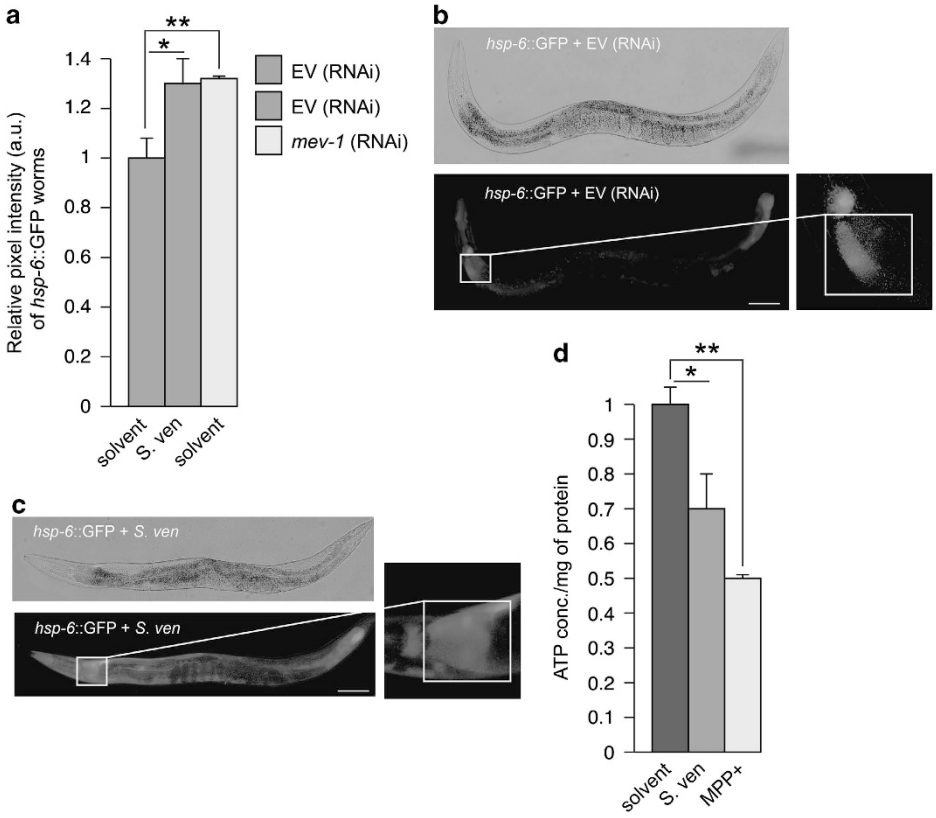

Figure 3 *S. venezuelae* metabolite causes mitochondrial dysfunction. (**a**) *S. venezuelae* metabolite caused an upregulation of *hsp-6*::GFP, an indicator of UPR^{mt} stress response. In this experiment, expression of *hsp-6*::GFP in EV RNAi-treated worms exposed to metabolite was significantly increased compared with worms exposed to solvent only, as quantitated using pixel intensities as visualized in (**b** and **c**). When compared with metabolite exposure, RNAi knockdown of *mev-1*, used as a positive control, expressed similar levels of *hsp-6*::GFP. Values are the mean ± S.D. of 3 experiments where 30 animals were analyzed per replicate (*$P<0.05$; **$P<0.01$; one-way ANOVA). The values were normalized to the untreated solvent control. (**b** and **c**) Representative worm images (brightfield (top) and fluorescence (bottom)) for EtAc and metabolite treatments described in (**a**). Pixel intensities were measured in a 100 × 100 μm region in the intestinal lumen immediately posterior to the grinder of the pharynx. The region highlighted in the white box shows GFP expression driven by the *hsp-6* gene promoter that was measured in all animals and is magnified to the right. (**d**) *C. elegans* exposed to the *S. venezuelae* metabolite showed reduced ATP production compared with the solvent control; worms treated with 1 mM MPP +, which is known to reduce ATP levels, also demonstrated a similar effect (*$P<0.05$; **$P<0.01$; one-way ANOVA). Values are the mean ± S.D. of three independent experiments and were normalized to the untreated control. Magnification bar = 100 μm

When exposed to metabolite, LRRK-2 G2019S expressing worms displayed significantly more DA neurodegeneration than animals expressing GFP only in DA neurons (Figure 5e).

***S. venezuelae* metabolite potentiates 6-OHDA or rotenone-induced DA neurodegeneration.** Epidemiological studies indicate that idiopathic parkinsonism could result from a combination of various risk factors. Therefore, we asked whether exposure to toxicants used in PD models that induce mitochondrial dysfunction and oxidative stress, such as 6-OHDA and rotenone,[36] along with the *S. venezuelae* metabolite, would result in enhanced DA neurodegeneration. 6-OHDA inhibits mitochondrial complexes I and IV, whereas rotenone displays specificity for complex I.[9,25]

We first examined a combination of 6-OHDA and metabolite. *C. elegans* were incubated with the *S. venezuelae* metabolite for half the standard exposure time to enhance visualizing neuronal vulnerability to a secondary stressor, such as 6-OHDA, while not appreciably causing neurodegeneration with metabolite alone. In this metabolite-only exposure paradigm, ~80% of the population still displayed normal DA neurons (Figures 6a and b). Nematodes were exposed to the metabolite (or EtAc solvent control) and exposed to 6-OHDA for 1 h at late larval stage 4. Here, we observed that 48 h post 6-OHDA treatment, worms exposed to *S. venezuelae* metabolite and 6-OHDA did not show a significant degeneration compared with worms treated with 6-OHDA alone. However, after 72 h, this same treatment provided a significant degeneration with respect to the controls (Figures 6b–e).

We further investigated the combined effect of rotenone, a known complex I inhibitor, and *S. venezuelae* metabolite. Unlike the 6-OHDA regimen, worms were continuously exposed to rotenone or DMSO solvent from the L4 stage and analyzed at day 10 (Figure 6f). Co-exposure of the metabolite with rotenone enhanced DA neurodegeneration compared with metabolite or rotenone alone (Figures 6g–i). Together, these results suggest that mitochondrial respiratory chain activity is sensitive to the metabolite-induced toxicity. These data also suggest that exposure to more than one environmental/chemical risk factor has an additive effect on DA neurodegeneration.

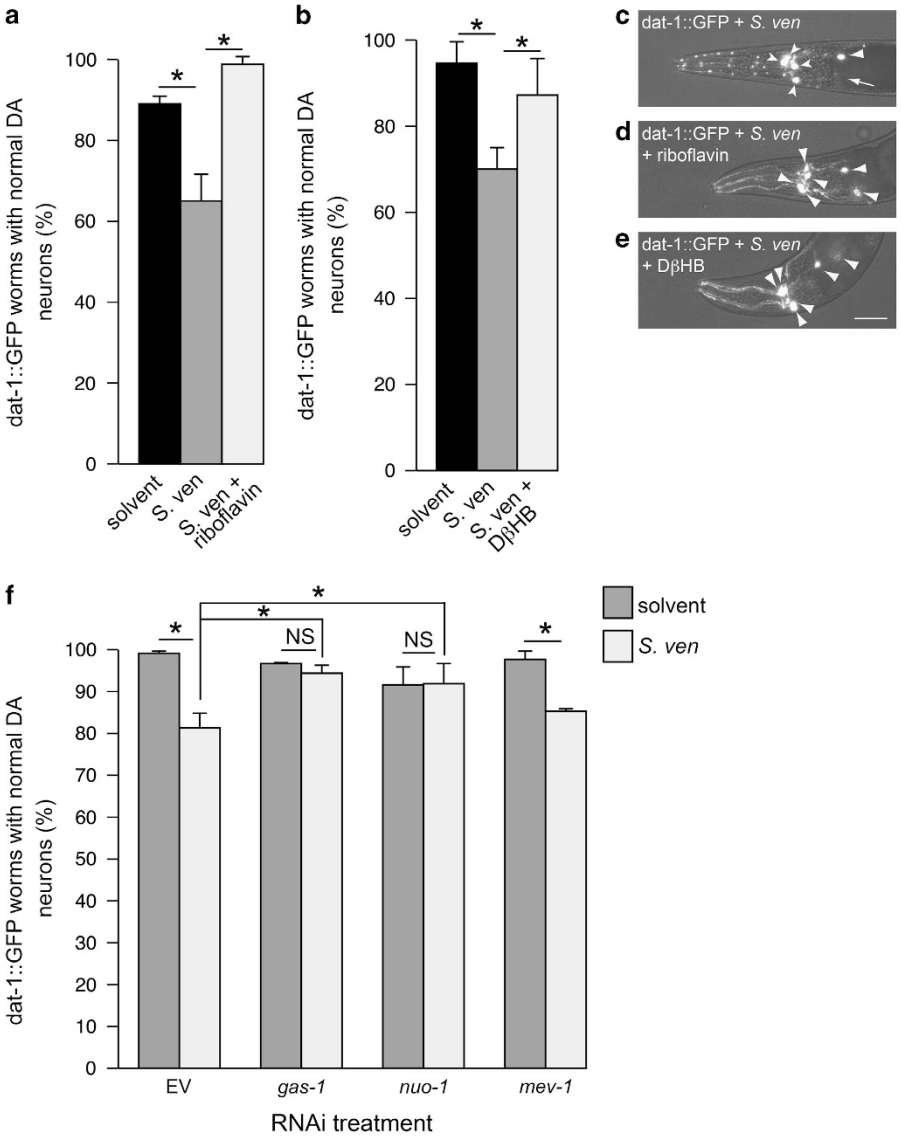

Figure 4 The *S. venezuelae* metabolite impacts mitochondrial complex I. (**a**–**e**) Metabolite-induced DA neurotoxicity was rescued by riboflavin and DβHB, drugs that rescue mitochondria complex I deficiency. (**a**) *S. venezuelae* and 1 μg/ml riboflavin significantly rescued DA neurons compared with the metabolite alone. (**b**) When 50 mM DβHB is co-administered with the metabolite, *C. elegans* DA neurons are rescued from neurotoxicity. (**c**–**e**) Representative images of riboflavin and DβHB rescuing DA neurotoxicity induced by the metabolite. All *C. elegans* (strain BY200) express GFP specifically in the six anterior DA neurons. In the images, large arrowheads show intact dopaminergic neuron cell bodies. Arrows indicate areas where dopaminergic neurons have degenerated. Small arrowheads indicate cell body degeneration. (**c**) Exposure to the *S. venezuelae* metabolite caused neuronal loss in this worm where five of the six DA neurons are degenerating. (**d**) The addition of riboflavin completely rescued DA neurons in an animal exposed to the metabolite. (**e**) DβHB also rescued *S. venezuelae*-induced DA neuronal toxicity, as shown in this *C. elegans* example. Magnification bar = 50 μm. (**f**) RNAi knockdown of complex I components *gas-1* and *nuo-1* resulted in rescue of DA neurodegeneration when treated with metabolite while complex II component *mev-1* and EV RNAi showed enhanced DA neurodegeneration with metabolite exposure (*$P<0.05$; one-way ANOVA; $n=90$ worms). *C. elegans* (strain UA202) were analyzed at day 12 where data were analyzed as the mean ± S.D.

Discussion

We previously reported an initial description of a highly stable and small molecular metabolite from *S. venezuelae* that caused *C. elegans* dopaminergic neurodegeneration and death of human SH-SY5Y neurons.[12] The impetus for that nascent work stemmed from our interest in what type of hypothetical and more common exposure could, in combination with misfortune in 'the genetic lottery', potentially account for the prevalence of PD – the second most common neurodegenerative disorder. However, while multi-hit hypotheses are attractive in clinically defining disease etiology, there remains little functional evidence for such scenarios. In this more mechanistic investigation, we exploit the advantages afforded through *C. elegans* research to combine genetic and toxicological analysis in a well-defined system that facilitates rapid and reproducible evaluation of neurodegeneration. We determined that the neurotoxic *S. venezuelae* metabolite caused excessive production of free oxygen radicals, upregulated the UPR^{mt}, and impaired mitochondrial complex I activity (Figure 7).

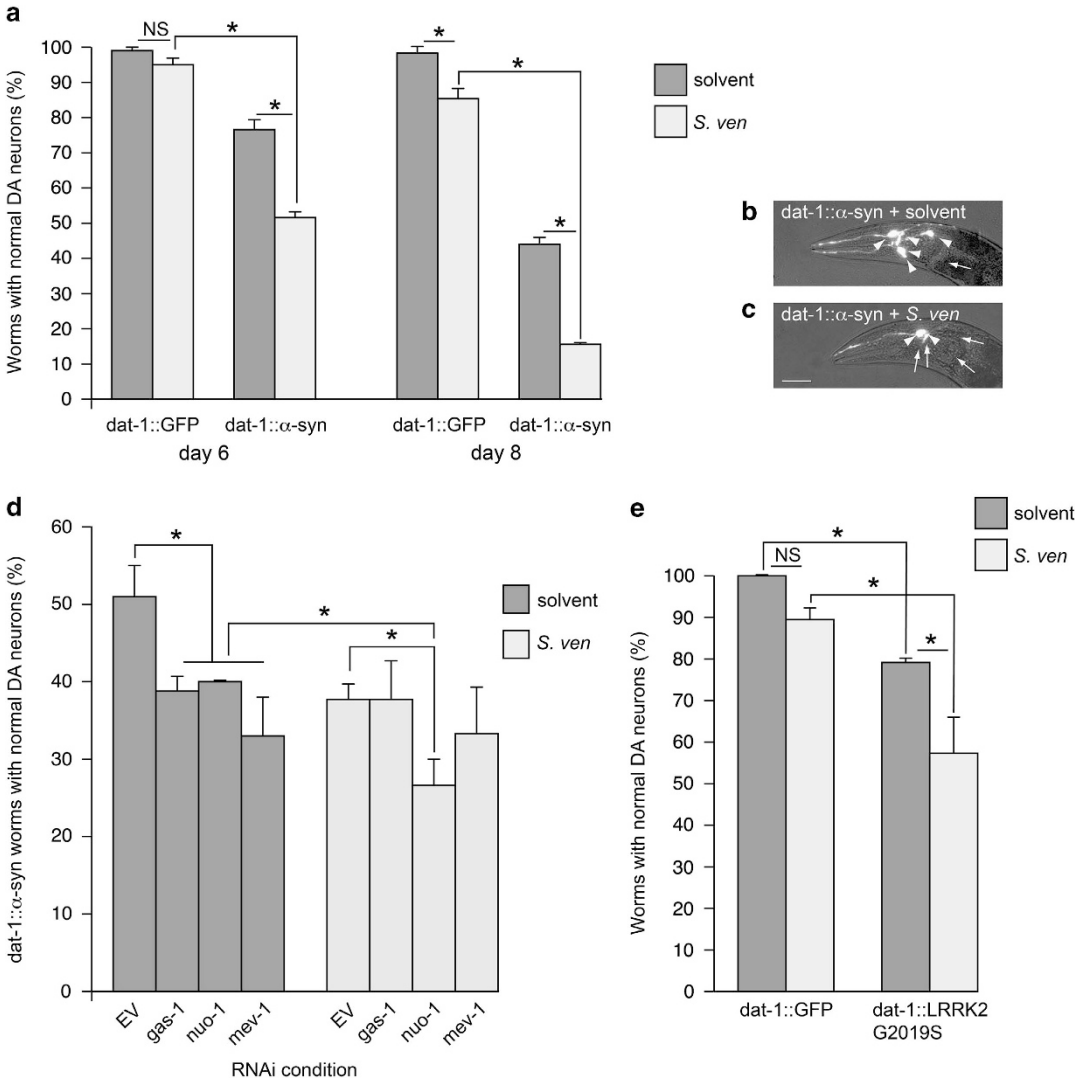

Figure 5 Gene and environment interaction enhances DA neurodegeneration. A combination of exposure to *S. venezuelae* and overexpression of known Parkinson's gene products, α-syn (**a**–**d**) or LRRK2 G2019S (**e**) enhances DA neurodegeneration. (**a**) *C. elegans* expressing GFP alone exhibit metabolite-induced age-dependent DA neurodegeneration that is evident when examining day 6 *versus* day 8 animals. Worms overexpressing α-syn display age-dependent DA neurodegeneration and are also more susceptible to metabolite-induced DA neurotoxicity when compared with populations of α-syn-expressing worms treated with solvent only. These data are represented as the mean ± S.D. $n = 90$ per data point (*$P < 0.05$ by one-way ANOVA). (**b** and **c**) Representative images of *C. elegans* (strain UA44) expressing α-syn and GFP specifically in the six anterior DA neurons in solvent (**b**) or in combination with metabolite exposure (**c**). In the images, large arrowheads show intact dopaminergic neuron cell bodies. Arrows indicate areas where dopaminergic neurons have degenerated. (**d**) RNAi knockdown of *gas-1*, *nuo-1*, and *mev-1* showed enhanced α-syn-induced DA neurodegeneration compared with α-syn alone without metabolite exposure. *C. elegans* (strain UA196) were analyzed at day 6 where data were analyzed as the mean ± S.D. After metabolite exposure, *nuo-1* RNAi-treated worms showed a significant sensitivity in worms expressing α-syn compared with EV (RNAi) metabolite-treated worms and *nuo-1* (RNAi) solvent control worms, whereas RNAi of *gas-1* and *mev-1* failed to cause a significant degeneration with metabolite treatment when compared with untreated controls (*$P < 0.05$; one-way ANOVA). (**e**) Metabolite-treated worms expressing GFP alone do not display a significant DA neurodegeneration when compared with solvent control at 7 days of exposure. Susceptibility to metabolite-induced DA neurotoxicity is enhanced when *C. elegans* overexpress human LRRK2 G2019S when compared with populations of worms treated with solvent only. Data are represented as the mean ± S.D., $n = 90$ per independent transgenic line; where three separate transgenic lines were analyzed (*$P < 0.05$ by one-way ANOVA). Magnification bar = 50 μm

Defects in mitochondria have long been known to contribute to neurodegeneration. Mitochondrial damage is more deleterious in neurons than other cell types as they are non-mitotic, have high metabolic activity, and low antioxidant capacity.[37] Using an oxidative stress inducible reporter, *sod-3*::GFP, we determined that the *S. venezuelae* metabolite increased ROS *in vivo* by measuring GFP levels within intestinal cells. These data are correlated with ROS production within whole animal extracts, as assayed biochemically using DCF-DA, where ROS was also upregulated in response to metabolite exposure. Finally, since we were interested in knowing whether the neurotoxicity associated with the metabolite was related to ROS, we treated *C. elegans* with an antioxidant, probucol, and assayed for DA neurodegeneration following metabolite exposure. Probucol protected these animals from neurodegeneration, thus providing further evidence that the metabolite elicits its toxicity at least partly through increased ROS production.

An accumulation of ROS can trigger the UPR^{mt}, a stress-response pathway that activates transcription of mitochondrial chaperone genes to promote protein homeostasis. The metabolite-induced activation of the UPR^{mt} that we observed using a worm strain expressing *hsp-6*::GFP was suggestive of a disturbance of mitochondrial homeostasis. Importantly, we previously demonstrated that the metabolite failed to activate *hsp-4*::GFP, an indicator of endoplasmic reticulum-induced UPR (UPR^{ER}).[12] Thus, our findings suggest that the UPR response triggered by *S. venezuelae* metabolite is mitochondrial specific. The mitochondrial protein-folding environment can be perturbed by any changes in the organelle structure, excess production of free radicals, and/or improper function of the electron transport chain.[21] The neurotoxicity we document in *C. elegans* is coincident with increased ROS generation and depletion of ATP levels, both of which imply mitochondrial dysfunction (Figure 7).

More detailed investigation of the mitochondrial impairment caused by the *S. venezuelae* metabolite highlighted impairment of complex I. Using activators of mitochondrial complex I, riboflavin and DβHB, DA neurodegeneration resulting from the metabolite was rescued. Riboflavin has been shown to improve both complex I and complex IV (cytochrome c oxidase) activity[28,38] whereas DβHB rescues complex I through complex II.[27] DβHB has been also shown to protect mouse DA neurons by mitigating the detrimental effects of complex I inhibition.[27] Worms treated with RNAi to knockdown complex I genes and the metabolite did not display neurodegeneration, further suggesting that the metabolite might target mitochondrial complex I. However, further investigation will include the direct measurement of complex I–IV enzymatic activities to confirm the direct target, or targets, of the metabolite. Currently, the compound we are utilizing in our studies could be a mixture of more than one metabolite. Efforts are underway to purify the neurotoxic molecule for future investigations.

Current literature suggests a reciprocal relationship between mitochondria and the ubiquitin proteasome system (UPS).[39] Metabolic function of the UPS impacts the regulation of mitochondrial dynamics, wherein functional perturbations in one of these systems affect the other. More specifically,

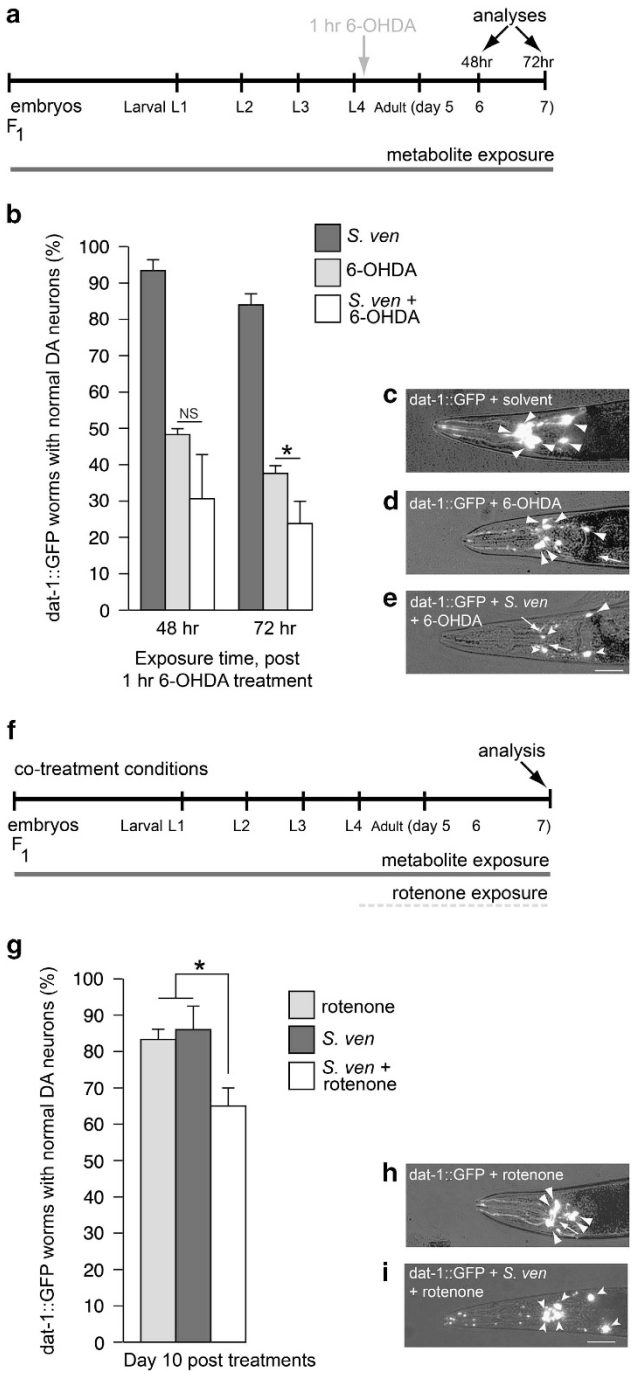

Figure 6 Hypersensitivity to *S. venezuelae* DA neurotoxicity when worms are treated with rotenone or 6-OHDA. (**a**) A timeline representing an experimental paradigm depicting the length of *S. venezuelae* metabolite exposure and 6-OHDA treatment. The abbreviations L1–L4 are the larval stages of *C. elegans,* while the 'adult' designations represent days post hatching. The 48 and 72 h represents times, post 1 h 6-OHDA (30 mM) treatment when DA neurons were analyzed. (**b**) At 48 h after 6-OHDA treatment, co-treatment with metabolite was not significantly different from individual treatments alone. Whereas, after 72 h, *C. elegans* co-exposed with the metabolite and 6-OHDA displayed significantly more susceptibility to DA neurodegeneration than either treatment alone (*$P<0.05$; one-way ANOVA; $n=90$ per treatment). (**c**–**e**) Representative images of *C. elegans* (strain BY200) expressing GFP specifically in the six anterior DA neurons. In the images, large arrowheads show intact dopaminergic neuron cell bodies. Arrows indicate areas where dopaminergic neurons have degenerated. Small arrowheads indicate cell body degeneration. (**c**) A control worm exposed to EtAc solvent only (no 6-OHDA or metabolite) has six normal DA neurons in the anterior region. (**d**) This representative worm exposed to 6-OHDA is missing one neuron. (**e**) In this example, a worm exposed to both 6-OHDA and the metabolite is missing two neurons while another three neurons display cell body rounding, indicative of degeneration. Magnification bar = 50 μm. (**f**) A timeline representing the experimental paradigm for a combination of *S. venezuelae* metabolite and rotenone exposure scored for DA neurodegeneration. The abbreviations are described in (**a**). (**g**) *C. elegans* co-exposed with the metabolite and 5 μM rotenone (in 0.05% DMSO) display significantly more susceptibility to DA neurodegeneration than either treatment alone (*$P<0.01$; Student's *t*-test; $n=90$ per treatment). (**h** and **i**) Representative images of *C. elegans* (strain BY200) expressing GFP specifically in the six anterior DA neurons. In the images, large arrowheads show intact dopaminergic neuron cell bodies. Arrows indicate areas where dopaminergic neurons have degenerated. Small arrowheads indicate cell body degeneration. (**h**) This representative worm exposed to rotenone was missing one neuron. (**i**) In this representative worm exposed to both rotenone and the metabolite, all neurons display cell body rounding, indicative of degeneration. Magnification bar = 50 μm

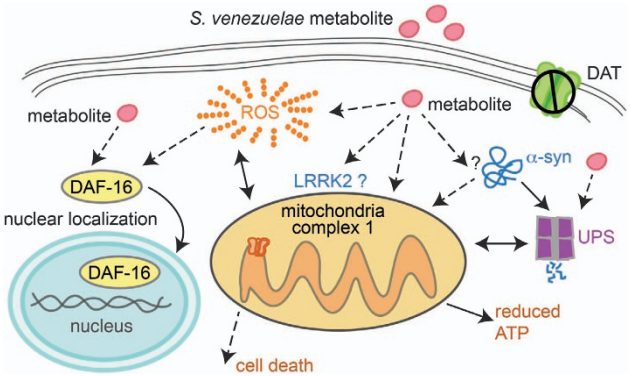

Figure 7 Experimental model for *S. venezuelae* metabolite-induced toxicity. This tentative model depicts our current understanding of the cellular mechanisms impacted. We previously determined that this metabolite does not enter cell membranes through the DA transporter, DAT.[12] It is possible that the metabolite diffuses through the cellular membrane because the initial biochemical structural characterization and purification efforts have shown that the molecule is small and highly lipophilic.[12] However, an unknown receptor could also be transducing a signal cascade. Regardless, we observe enhanced oxidative stress in response to metabolite exposure. The excessive production of ROS by the metabolite could be a direct result of redox cycling *in vivo* or it could be the result of mitochondrial dysfunction. There could also be a reciprocal relationship between ROS and mitochondrial dysfunction following metabolite exposure. Alternatively, the metabolite could directly target mitochondrial complex I, leading to ATP production impairment, upregulation of the UPR^{mt}. These cellular responses could trigger cell death. Additionally, the metabolite could activate the FOXO transcription factor DAF-16 directly or as a secondary cellular response to ROS production. Furthermore, based on our DA neurodegeneration studies, there might be a direct or indirect association between the *S. venezuelae* metabolite and α-synuclein or LRRK2 in targeting mitochondria. We have previously reported that the metabolite inhibits the UPS.[12] Considering that proteasome function intersects with the various mechanisms described in this model, future studies will explore this functional association.

mitochondrial complex I activity has been linked with UPS function.[40] Previously, we have reported that *S. venezuelae* metabolite inhibits the UPS.[12] Thus, the bacterial metabolite seems to be involved in several intersecting pathways associated with neurodegeneration, including oxidative stress, mitochondrial dysfunction, and proteasomal dysfunction/protein aggregation. The exact mechanistic order underlying toxicity is yet to be determined. It is possible that UPS inhibition is either a consequence of direct proteasome inhibition by the metabolite or is indirectly caused by mitochondrial impairment or oxidative damage from ROS. Conversely, proteasome inhibition might in turn affect mitochondrial respiration (Figure 7). It is notable that in our genetic studies the effect of the metabolite appears to be enhanced in the presence of α-syn. Complex I and II gene knockdowns in an α-syn sensitized background uncovered a hypersensitivity of the complex I component, *nuo-1*, to the metabolite, suggesting that DA neurons are more susceptible to degenerative stressors. Thus, under conditions where protein homeostasis is already out of balance, a direct or indirect relationship between the bacterial metabolite and α-syn may result in mitochondrial dysfunction.

Oxidative stress and mitochondrial dysfunction are also two inseparable elements of PD, where mitochondria are a common target of several genetic and environmental risk factors. In this regard, our results on the combined neurotoxic effect of 6-OHDA, rotenone, or familial risk factors for PD with the *S. venezuelae* metabolite support a multiple-hit contribution to dopaminergic neurodegeneration. For example, others and we have shown a relationship between Mn++ toxicity, α-syn misfolding, and lysosomal dysfunction associated with the ATP13A2/PARK9 gene product.[41] Similarly, overexpression of LRRK2 mutations in *C. elegans* is associated with changes in mitochondrial function and autophagy.[42] In this study, we found metabolite-enhanced neurodegeneration of *C. elegans* expressing LRRK2 G2019S. This was reminiscent of results in other model organisms where expression of mutant LRRK2 is associated with increased sensitivity to rotenone.[43] Several familial forms of PD have identified gene mutations that cause mitochondrial dysfunction, including parkin, PINK1, and DJ-1; studies designed to evaluate combined impact of the metabolite with these mutations are in progress.

In considering potential mechanisms that could trigger an oxidative stress response, we discerned that the *S. venezuelae* metabolite caused the FOXO transcription factor protein, DAF-16, to translocate to the nucleus in a manner similar to what has been reported in response to paraquat.[44] We conclude that this nuclear accumulation caused by the metabolite relates to increased intracellular ROS and may be under the control of a genetic program to combat pathogens, sense mitochondrial dysfunction or promote cell death.[13,45–47] DAF-16, along with SKN-1, are transcription factors that work in parallel and are directly inhibited by the insulin-signaling pathway. Each transcription factor contributes to stress resistance and has a set of target genes, some of which are overlapping. It is interesting to note that following exposure to the *S. venezuelae* metabolite, *C. elegans* expressing a reporter for SKN-1 did not exhibit activation, in contrast to results reported for exposure to paraquat.[48] While beyond the scope of this study, future research will explore DAF-16 targets of the metabolite. A recent study described a genome-wide RNAi screen for gene products that were upregulated in a UPR^{mt} readout in *C. elegans* following paraquat exposure.[49] Considering that most, but not all cellular readouts are identical following metabolite and paraquat treatments in *C. elegans*, it would be interesting to examine newly identified regulators of ROS-induced UPR^{mt}.

In conclusion, we report that the *S. venezuelae* metabolite shares common molecular mechanisms with other PD toxicants that cause DA neurodegeneration, such as impairment of mitochondrial complex 1 and upregulation of the UPR^{mt}. These studies advance our understanding of DA neurodegeneration and as well provide an additional model for analysis of PD-associated pathogenesis.

Materials and Methods

***C. elegans* strains.** Nematodes were maintained using standard procedures.[50] We obtained the following strains from CGC: TJ356 [*zIs356* (P_{daf-16}::DAF-16::GFP; *rol-6*(su1006))], LD1 [*ldIs7*{P_{skn-1}::skn-1B/C::GFP + pRF4(*rol-6*(su1006))}], SJ4100 [*zcIs13*(P_{hsp-6}::GFP)], and KN259 [*huIs33*{sod-3::GFP + pRF4(*rol-6*(su1006))}]. Strain BY200 [*vtIs1*{P_{dat-1}::GFP, pRF4(*rol-6*(su1006))}] and BY250 [*vtIs7*; P_{dat-1}::GFP] were generous gifts from Randy Blakely (Vanderbilt University). The strain UA44 [*baIn1*; P_{dat-1}::α-syn, P_{dat-1}::GFP] expresses α-syn and GFP in the DA neurons. UA202 [*sid-1* (pk3321); *baIn33* (P_{dat-1}::*sid-1*, P_{myo-2}::mCherry); (P_{dat-1}::GFP)] expresses GFP and SID-1 in the DA neurons. UA196 [*sid-1*(pk3321); *baIn33* (P_{dat-1}::*sid-1*, P_{myo-2}::mCherry);

($P_{dat\text{-}1}$::α-syn, $P_{dat\text{-}1}$::GFP)] expresses α-syn, GFP, and SID-1 in the DA neurons.[30,51] UA202 and UA196 strains are sensitive to RNAi specifically in the DA neurons. $P_{dat\text{-}1}$::LRRK2 G2019S plasmids were co-injected into the gonads of strain BY250 [*vtIs7*; $P_{dat\text{-}1}$::GFP] to generate UA215 [*baEx128*; $P_{dat\text{-}1}$::LRRK2 G2019S; *vtIs7*($P_{dat\text{-}1}$::GFP)].[52]

Isolation and extraction of *S. venezuelae* metabolite. Spores from *S. venezuelae* strain (ARS NRRL ISP-5230) were inoculated in 5 liters of SYZ media at a density of 1×10^8 and were grown at 30°C in a shaker. Samples were harvested at ~20 days when cell density became constant. Cell debris was removed by centrifugation at 10 000 *g* for 10 min and supernatants were sequentially passed through eight PES filter membranes with the following pore sizes: 11, 6, 2.7, 1.7, 1.2, 0.7, 0.45, and 0.22 μm. After filtration, the conditioned media was extracted with an equal volume of DCM using a separatory funnel. The mixture was gently shaken and the phases were allowed to separate overnight. The DCM layer was collected and the process was repeated two more times. The organic phases were pooled together, dried, and resuspended in 1 ml of EtAc. For all worm assays, 25 μl/ml of partially purified *S. venezuelae* medium or 25 μl/ml EtAc (solvent control) was added to the surface of nematode growth medium (NGM) Petri plates along with *E. coli* (strain OP50).

***C. elegans* neurodegeneration assay.** Adult $P_{dat\text{-}1}$::GFP animals (strain BY200 or strain BY250), $P_{dat\text{-}1}$::α-syn (strain UA44), or $P_{dat\text{-}1}$::LRRK2 G2019S (strain UA215) was placed on plates with *S. venezuelae* metabolite and allowed to lay eggs for ~4 h, before the adults were removed. The worm embryos were grown under constant exposure to partially purified *S. venezuelae* metabolite or EtAc (solvent control) until the day of analysis. Worms were transferred to freshly made plates every other day and a total of 30–40 worms were scored for neurodegeneration after 6, 8, 10, or 12 days of metabolite exposure (3-, 5-, 7-, or 9-day-old adults). Worms were considered as normal when all six anterior dopaminergic neurons (two ADE (anterior deirid) and four CEP (cephalic)) were intact and no visible signs of degeneration were observed. If a worm displayed a neuron with any degenerative change (missing neuronal processes, rounding or cell body loss, or blebbing process), then it was scored as exhibiting a degenerative phenotype. The $P_{dat\text{-}1}$::GFP animals (strains BY200 and BY250) and $P_{dat\text{-}1}$::α-syn (strain UA44) animals have chromosomally integrated transgenes where a single isogenic line was used for analyses in all experiments. The LRRK2 G2019S transgene in strain UA215 remains as extrachromosomal arrays. Therefore, three independent lines of transgenic worms were analyzed and an average of total percentage of worms with neurodegeneration was reported for these experiments.

RNAi treatments for neurodegeneration assay. The *mev-1* (T07C4.7), *nuo-1* (C09H10.3), *gas-1* (K09A9.5), and L4440 (EV control) RNAi feeding constructs were obtained from the *C. elegans* Ahringer library.[53] These RNAi bacterial feeding clones were isolated and grown overnight in LB media containing 100 μg/ml ampicillin. Small NGM plates (4 ml worm agar media) containing 1 mM IPTG were seeded with 250 μl RNAi culture and allowed to dry overnight. Next day, equal concentration (25 μl/ml) of partial purified *S. venezuelae* metabolite and EtAc (solvent control) were added to the respective plates. Ten dauer worms (DA neuron-specific RNAi worm strains, UA202 and UA196) were transferred to the plates and grown at 20°C for 48 h. Adult worms were then transferred to another set of freshly made RNAi + metabolite or RNAi + EtAc plates and allowed to lay eggs for 6 h to synchronize. The DA neurons in the F_1 progeny of the RNAi-treated worms were analyzed at day 6 or day 12 for neurodegeneration, as described above.

Semi-acute dosage of animals bearing fluorescent reporters. For *sod-3*::GFP, *hsp-6*::GFP, *daf-16*::GFP and *skn-1*::GFP reporter assay, a mixture of L3 and L4 staged animals from each genotype were placed onto small NGM plates with 0.4% β-lactose and ampicillin plates seeded with 250 μl RNAi bacteria: L4440 EV as a control or *mev-1* (T07C4.7) for UPR stress response assay or *daf-2* (Y55D5A.5) for oxidative stress assays. These RNAi strains were obtained from Ahringer *C. elegans* library.[53] Each plate was supplemented with an equal concentration (25 μl/ml) of partial purified *S. venezuelae* metabolite or EtAc (solvent control). This initial propagation is to establish a generational exposure to the metabolite *in utero*. Worms were then allowed to hatch and synchronize at L1 stage for 10–12 h. Next, animals were collected in 10 ml conical glass tubes, washed with M9 buffer and spun down at 10 000 *g* for 10 min. After the supernatant was removed, a final concentration (25 μl/ml) of metabolite or EtAc was added to the tubes, followed by gentle shaking for 8 h. This treatment establishes an acute pulse of dosage followed by chronic exposure. The treated worms were placed on respective RNAi plates and were analyzed at 60 h post treatment (young adult worms).

Quantification of ROS. Intracellular ROS were measured in *C. elegans* using DCF-DA (C-369, Life Technologies, Carlsbad, CA, USA) as described previously.[15] Stock solution of 20 mM DCF-DA dissolved in DMSO was stored in −20°C. A total of 30 age-synchronized wild-type worms were collected in microcentrifuge tubes after 7, 10, and 12 days of EtAc or metabolite or 100 μM paraquat exposure. After washing with M9 buffer (for 1 l: 3 g KH_2PO_4, 6 g Na_2HPO_4, 5 g NaCl, 1 ml $MgSO_4$) the worms were suspended into 100 μl of PBS with 1% Tween-20 (PBST). The worms were then subjected to repeated freeze-thaw cycling and sonication to rupture the outer cuticle. The worm lysates were then collected to 96-well plates. A final concentration of 50 nM DCF-DA in 100 μl PBS was added to each well. ROS-associated fluorescence levels were measured kinetically using SpectraMax M2e Microplate Reader (Molecular Devices, Sunnyvale, CA, USA) at excitation wavelength of 485 nm and emission wavelength of 530 nm, room temperature, every 20 min for 2.5 h. Data were normalized to solvent control. ROS measurements were conducted on three independent replicates and are presented as means ± S.D.

6-OHDA and rotenone assay. 6-OHDA assay was performed as previously described.[54] Metabolite- and EtAc-treated L4 worms (BY200) were washed with ddH_2O three times, and treated with 30 mM 6-OHDA (Tocris Bioscience, Bristol, UK) containing 1 mM ascorbic acid, followed by gentle agitation for 1 h. Subsequently, the worms were again washed and put onto freshly made metabolite or EtAc plates until analysis. For rotenone assay, BY200 worms were exposed to the metabolite or EtAc until L4 and then transferred to plates containing metabolite, along with 5 μM of rotenone or DMSO (as a solvent control for rotenone).

ATP measurements. The ATP assay was performed as described before,[55] with minor modifications. Worms were grown on metabolite or EtAc and collected for assay. As a positive control, EtAc-treated worms were soaked in 1 mM MPP + (Sigma, Santa Ana, CA, USA) for 1 h, left on seeded plates for 4–5 h to recover and then collected. In all, 100 age-synchronized young adult wild-type worms were washed with M9 buffer, treated with three free-thaw cycles and boiled for 15 min to release ATP and destroy ATPase activity. Samples were then spun at 4°C, 11 000 *g* for 10 min. A Life Technologies ATP determination kit (Molecular Probes, Eugene, OR, USA, A22066), which utilizes luciferase to catalyze the formation of light from ATP-dependent oxidation of D-luciferin, was used to quantify ATP contents. ATP concentrations were determined using standard curve derived from bioluminescence of known ATP concentrations. A single-tube luminometer (GloMax 20/20; Promega, Madison, WI, USA) was used to measure levels of bioluminescence. For normalization, protein levels were determined by a BCA protein assay kit (Pierce, Thermo Scientific, Rockford, IL, USA).

Drug treatment. A final concentration of 100 μM Paraquat (Sigma), 1 μg/ml Riboflavin (Calbiochem, EMD Bioscience, San Diego, CA, USA), 1 mM Probucol (MP Biomedicals, St. Louis, MO, USA), and 50 mM DβHB (Sigma-Aldrich, St. Louis, MO, USA) were supplemented in the worm media for their respective experiments. The *S. venezuelae* metabolite or EtAc was added to these plates before use.

Quantitative fluorescence measurements and statistics. Worms were immobilized with 3 mM levamisole and mounted on 2% agarose pads on a microscope slide. Fluorescent microscopy was performed using a Nikon Eclipse E800 epifluorescence microscope equipped with an Endow GFP HYQ filter cube (Chroma Technology, Bellows Falls, VT, USA). A Cool Snap CCD camera (Photometrics, Tucson, AZ, USA) driven by the MetaMorph software (Molecular Devices) was used to acquire images. Each animal was imaged in the same region at the same magnification and exposure intensity as previously described.[56] When analyzing each animal, a 100 × 100 μm box was used in the same region of the animal. For the *sod-3* transcriptional fusion reporter, this area was the region at the anterior bulb of the pharynx. For the *hsp-6* transcriptional fusion reporter, this area was the intestinal lumen immediately posterior to the grinder of the pharynx. Pixel intensity was quantified in this manner and compiled across

three-four separate replicates. For DAF-16 experiment, the entire animal was observed. If no nuclear accumulation could be seen, then it was scored as cytoplasmic, if some, accumulation was observed then it was scored as both, and if robust, nuclear accumulation could be observed throughout the animal then it was scored as nuclear. For the SKN-1 experiment, a dual red-green filter was used to observe emerging green fluorescence from the intestine over the background fluorescence of gut granules (which appear yellow). A similar scoring system was used to that of DAF-16. For statistical analysis, a one-way ANOVA followed by *post hoc* Tukey's or Dunnett's test was employed for comparison of more than two data sets (Prism 6.0 software; GraphPad, La Jolla, CA, USA). For comparisons between two data sets, Student's *t*-test was performed. All the experiments were performed with three independent replicates and are presented as means $\pm$ S.D. A value of $P \leq 0.05$ or $P \leq 0.01$ is considered as statistically significant.

Conflict of Interest

The authors declare no conflict of interest.

Acknowledgements. We would like to thank all members of the Caldwell laboratory for their creative and collegial nature. We would also like to thank Julie Olson, Tyler Hodges, Janna Brown, and Robert Findlay for collaborative assistance in prior experimental acquisition and partial purification of the *S. venezuelae* metabolite. The Caenorhabditis Genetics Center (CGC), which is funded by NIH Office of Research Infrastructure Programs (P40 OD010440), provided *C. elegans* strains. This research was funded by NIH grant R15NS074197-01 to KAC.

1. Spillantini MG, Schmidt ML, Lee VM, Trojanowski JQ, Jakes R, Goedert M. Alpha-synuclein in Lewy bodies. *Nature* 1997; **388**: 839–840.
2. Tanner CM. Is the cause of Parkinson's disease environmental or hereditary? Evidence from twin studies. *Adv Neurol* 2003; **91**: 133–142.
3. Priyadarshi A, Khuder SA, Schaub EA, Priyadarshi SS. Environmental risk factors and Parkinson's disease: a meta-analysis. *Environ Res* 2001; **86**: 122–127.
4. Costello S, Cockburn M, Bronstein J, Zhang X, Ritz B. Parkinson's disease and residential exposure to maneb and paraquat from applications in the central valley of California. *Am J Epidemiol* 2009; **169**: 919–926.
5. Liou HH, Tsai MC, Chen CJ. Environmental risk factors and Parkinson's disease: a case-control study in Taiwan. *Neurology* 1997; **48**: 1583–1588.
6. Greenamyre JT, MacKenzie G, Peng TI, Stephans SE. Mitochondrial dysfunction in Parkinson's disease. *Biochem Soc Symp* 1999; **66**: 85–97.
7. Gorell JM, Johnson CC, Rybicki BA, Peterson EL, Richardson RJ. The risk of Parkinson's disease with exposure to pesticides, farming, well water, and rural living. *Neurology* 1998; **50**: 1346–1350.
8. Yano K, Yokoi K, Sato J, Oono J, Kouda T, Ogawa Y *et al.* Actinopyrones A, B and C, new physiologically active substances. II. Physico-chemical properties and chemical structures. *J Antibiot* 1986; **39**: 38–43.
9. Thiffault C, Langston JW, Di Monte DA. Increased striatal dopamine turnover following acute administration of rotenone to mice. *Brain Res* 2000; **885**: 283–288.
10. Lotharius J, O'Malley KL. The Parkinsonism- inducing drug 1-methyl-4-phenylpyridinium triggers intra- cellular dopamine oxidation: a novel mechanism of toxicity. *J Biol Chem* 2000; **275**: 38581–38588.
11. Cocheme HM, Murphy MP. Complex I is the major site of mitochondrial superoxide production by paraquat. *J Biol Chem* 2008; **283**: 1786–1798.
12. Caldwell KA, Tucci ML, Armagost J, Hodges TW, Chen J, Memon SB *et al.* Investigating bacterial sources of toxicity as an environmental contributor to dopaminergic neurodegeneration. *PLoS One* 2009; **4**: e7227.
13. Essers MAG, Vries-Smits LMM, Barker N, Polderman PE, Burgering BMT, Korswagen HC. Functional interaction between β-Catenin and FOXO in oxidative stress signaling. *Science* 2005; **308**: 1181–1184.
14. Libina N, Berman JR, Kenyon C. Tissue-specific activities of C. elegans DAF-16 in the regulation of lifespan. *Cell* 2003; **115**: 489–502.
15. Wu Y, Wu Z, Butko P, Christen Y, Lambert MP, Klein WL *et al.* Amyloid-ß-induced pathological behaviors are suppressed by Ginkgo biloba extract EGb 761 and Ginkgolides in transgenic Caenorhabditis elegans. *J Neurosci* 2006; **26**: 13102–13113.
16. Honda Y, Honda S. The daf-2 gene network for longevity regulates oxidative stress resistance and Mn-superoxide dismutase gene expression in Caenorhabditis elegans. *FASEB J* 1999; **13**: 1385–1393.
17. Henderson ST, Johnson TE. daf-16 integrates developmental and environmental inputs to mediate aging in the nematode Caenorhabditis elegans. *Curr Biol* 2001; **11**: 1975–1980.
18. Motohashi H, Yamamoto M. Nrf-2-Keap-1 defines a physiologically important stress response mechanism. *Trends Mol Med* 2004; **10**: 549–557.
19. An JH, Blackwell TK. SKN-1 links C. elegans mesendodermal specification to a conserved oxidative stress response. *Genes Dev* 2003; **17**: 1882–1893.
20. Hoeven Rv McCallum KC, Cruz MR, Garsin DA. Ce-Duox1/BLI-3 generated reactive oxygen species trigger protective SKN-1 activity *via* p38 MAPK signaling during infection in C. elegans. *PLoS Pathog* 2011; **7**: e1002453.
21. Haynes CM, Ron D. The mitochondrial UPR- protecting organelle protein homeostasis. *J Cell Sci* 2010; **123**: 3849–3855.
22. Yoneda T, Benedetti C, Urano F, Clark SG, Harding HP, Ron H. Compartment-specific perturbation of protein handling activates genes encoding mitochondrial chaperones. *J Cell Sci* 2004; **117**: 4055–4066.
23. Durieux J, Wolff S, Dillin A. The cell non-autonomous nature of electron transport chain-mediated longevity. *Cell* 2011; **144**: 79–91.
24. Wang YM, Pu P, Le WD. ATP depletion is the major cause of MPP + induced dopamine neuronal death and worm lethality in alpha-synuclein transgenic C. elegans. *Neurosci Bull* 2007; **23**: 329–335.
25. Glinka YY, Youdim MB. Inhibition of mitochondrial complexes I and IV by 6-hydroxydopamine. *Eur J Pharmacol* 1995; **292**: 329–332.
26. Betarbet R, Sherer TB, MacKenzie G, Garcia-Osuna M, Panov AV, Greenamyre JT. Chronic systemic pesticide exposure reproduces features of Parkinson's disease. *Nat Neurosci* 2000; **3**: 1301–1306.
27. Tieu K, Perier C, Caspersen C, Teismann P, Wu DC, Yan SD *et al.* D-beta-hydroxybutyrate rescues mitochondrial respiration and mitigates features of Parkinson disease. *J Clin Invest* 2003; **112**: 892–901.
28. Grad LI, Lemire BD. Mitochondrial complex I mutations in Caenorhabditis elegans produce cytochrome c oxidase deficiency, oxidative stress and vitamin-responsive lactic acidosis. *Hum Mol Genet* 2004; **13**: 303–314.
29. Ved R, Saha S, Westlund B, Perier C, Burnam L, Sluder A *et al.* Similar patterns of mitochondrial vulnerability and rescue induced by genetic modification of α-Synuclein, Parkin, and DJ-1 in Caenorhabditis elegans. *J Biol Chem* 2005; **280**: 42655–42668.
30. Harrington AJ, Yacoubian TA, Slone SR, Caldwell KA, Caldwell GA. Functional analysis of VPS41-mediated neuroprotection in Caenorhabditis elegans and mammalian models of Parkinson's disease. *J Neurosci* 2012; **32**: 2142–2153.
31. Devi L, Raghavendran V, Prabhu BM, Avadhani NG, Anandatheerthavarada HK. Mitochondrial import and accumulation of alpha-synuclein impair complex I in human dopaminergic neuronal cultures and Parkinson disease brain. *J Biol Chem* 2008; **283**: 9089–9100.
32. Hamamichi S, Rivas RN, Knight AL, Cao S, Caldwell KA, Caldwell GA. Hypothesis-based RNAi screening identifies neuroprotective genes in a Parkinson's disease model. *Proc Natl Acad Sci* 2008; **105**: 728–733.
33. Nakamura K, Nemani VM, Azarbal F, Skibinski G, Levy JM, Egami K *et al.* Direct membrane association drives mitochondrial fission by the Parkinson disease-associated protein α-Synuclein. *J Biol Chem* 2011; **286**: 20710–20726.
34. Mortiboys H, Johansen KK, Aasly JO, Bandmann O. Mitochondrial impairment in patients with Parkinson disease with the G2019S mutation in LRRK2. *Neurology* 2010; **75**: 2017–2020.
35. Saha S, Guillily MD, Ferree A, Lanceta J, Chan D, Ghosh J *et al.* LRRK2 modulates vulnerability to mitochondrial dysfunction in C. elegans. *J Neurosci* 2009; **29**: 9210–9218.
36. Cohen G, Heikkila RE. The generation of hydrogen peroxide, superoxide radical, and hydroxyl radical by 6-hydroxydopamine, dialuric acid, and related cytotoxic agents. *J Biol Chem* 1974; **249**: 2447–2452.
37. Exner N, Lutz AK, Haass C, Winklhofer KF. Mitochondrial dysfunction in Parkinson's disease: molecular mechanisms and pathophysiological consequences. *EMBO J* 2012; **31**: 3038–3062.
38. Grad LI, Lemire BD. Riboflavin enhances the assembly of mitochondrial cytochrome c oxidase in C. elegans NADH-ubiquinone oxidoreductase mutants. *Biochim Biophys Acta* 2006; **1757**: 115–122.
39. Radke S, Chander H, Schäfer P, Meiss G, Krüger R, Schulz JB *et al.* Mitochondrial protein quality control by the proteasome involves ubiquitination and the protease Omi. *J Biol Chem* 2008; **283**: 12681–12685.
40. Hoglinger GU, Carrard G, Michel PP, Medjaà F, Lombesà A, Ruberg M *et al.* Dysfunction of mitochondrial complex I and the proteasome: interactions between two biochemical deficits in a cellular model of Parkinson's disease. *J Neurochem* 2003; **86**: 1297–1307.
41. Gitler AD, Chesi A, Geddie ML, Strathearn KE, Hamamichi S, Hill KJ *et al.* Alpha-synuclein is part of a diverse and highly conserved interaction network that includes PARK9 and manganese toxicity. *Nat Genet* 2009; **41**: 308–315.
42. Di Domenico F, Sultana R, Ferree A, Smith K, Barone E, Perluigi M *et al.* Redox proteomics analyses of the influence of co-expression of wild-type or mutated LRRK2 and Tau on C. elegans protein expression and oxidative modification: relevance to Parkinson disease. *Antioxid Redox Signal* 2012; **17**: 1490–1506.
43. Ng CH, Mok SZ, Koh C, Ouyang X, Fivaz ML, Tan EK *et al.* Parkin protects against LRRK2 G2019S mutant-induced dopaminergic neurodegeneration in Drosophila. *J Neurosci* 2009; **29**: 11257–11262.
44. Kondo M, Yanase S, Ishii T, Hartman PS, Matsumoto K, Ishii N. The p38 signal transduction pathway participates in the oxidative stress-mediated translocation of DAF-16 to Caenorhabditis elegans nuclei. *Mech Ageing Dev* 2005; **126**: 642–647.
45. Chavez V, Mohri-Shiomi A, Maadani A, Vega LA, Garsin DA. Oxidative stress enzymes are required for DAF-16 mediated immunity due to generation of reactive oxygen species in Caenorhabditis elegans. *Genetics* 2007; **176**: 1567–1577.

46. Lehtinen MK, Yuan Z, Boag PR, Yang Y, Villén J, Becker EB *et al.* A conserved MST-FOXO signaling pathway mediates oxidative stress responses and extends lifespan. *Cell* 2006; **125**: 987–1001.
47. Jacobs KM, Pennington JD, Bisht KS, Aykin-Burns N, Kim HS, Mishra M *et al.* SIRT3 interacts with the daf-16 homolog FOXO3a in the mitochondria, as well as increases FOXO3a dependent gene expression. *Int J Biol Sci* 2008; **4**: 291–299.
48. Tullet JMA, Hertweck M, An JH, Baker J, Hwang JY, Liu S *et al.* Direct inhibition of the longevity promoting factor SKN-1 by Insulin-like signaling in C. elegans. *Cell* 2008; **132**: 1025–1038.
49. Runkel ED, Liu S, Baumeister R, Schulze E. Surveillance-activated defenses block the ROS-induced mitochondrial unfolded protein response. *PLoS Genet* 2013; **3**: e10003346.
50. Brenner S. The genetics of Caenorhabditis elegans. *Genetics* 1974; **77**: 71–94.
51. Calixto A, Chelur D, Topalidou I, Chen X, Chalfie M. Enhanced neuronal RNAi in C. elegans using SID-1. *Nat Methods* 2010; **7**: 554–559.
52. Liu Z, Hamamichi S, Lee BD, Yang D, Ray A, Caldwell GA *et al.* Inhibitors of LRRK2 kinase attenuate neurodegeneration and Parkinson-like phenotypes in C. elegans and Drosophila Parkinson's disease models. *Hum Mol Genet* 2011; **20**: 3933–3942.
53. Kamath RS, Fraser AG, Dong Y, Poulin G, Durbin R, Gotta M *et al.* Systematic functional analysis of the Caenorhabditis elegans genome using RNAi. *Nature* 2003; **421**: 231–237.
54. Nass R, Hall DH, Miller DM, Blakely RD. Neurotoxin-induced degeneration of dopamine neurons in Caenorhabditis elegans. *PNAS* 2002; **99**: 3264–3269.
55. Yang W, Hekimi S. A. Mitochondrial Superoxide Signal Triggers Increased Longevity in Caenorhabditis elegans. *PLoS Biol* 2010; **8**: e1000556.
56. Kimura K, Tanaka N, Nakamura N, Takano S, Ohkuma S. Knockdown of mitochondrial heat shock protein 70 promotes Progeria-like phenotypes in Caenorhabditis elegans. *J Biol Chem* 2007; **282**: 5910–5918.